

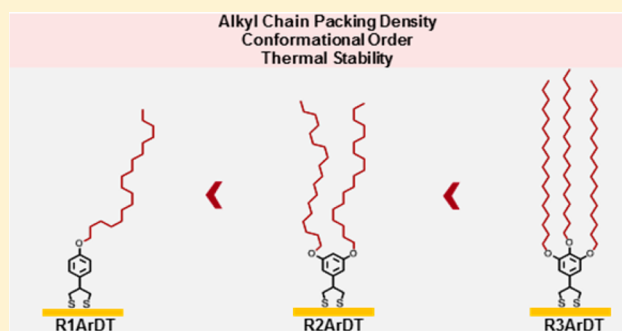
Bidentate Aromatic Thiols on Gold: New Insight Regarding the Influence of Branching on the Structure, Packing, Wetting, and Stability of Self-Assembled Monolayers on Gold Surfaces

Supachai Rittikulsittichai, Chul Soon Park, Andrew C. Jamison, Daniela Rodriguez, Oussama Zenasni, and T. Randall Lee*[✉]

Department of Chemistry and the Texas Center for Superconductivity, University of Houston, 4800 Calhoun Road, Houston, Texas 77204-5003, United States

Supporting Information

ABSTRACT: A series of 2-phenylpropane-1,3-dithiol derivatives with single (**R1ArDT**), double (**R2ArDT**), and triple (**R3ArDT**) octadecyloxy chains substituted at the 4-, 3,5-, and 3,4,5-positions, respectively, on the aromatic ring were synthesized and used to form self-assembled monolayers (SAMs) on gold. Insight into the relationship between the surface chain and headgroup packing densities was investigated by varying the number of surface chains for the bidentate adsorbates in these monolayers. Characterization of the resulting SAMs using ellipsometry, X-ray photoelectron spectroscopy, polarization modulation infrared reflection–absorption spectroscopy, and contact angle goniometry revealed that the tailgroups become more conformationally ordered and more densely packed as the number of alkyl chains per adsorbate was increased. Conversely, the molecular packing density (i.e., number of molecules per unit area) decreased as the number of alkyl chains per adsorbate was increased. Of particular interest, the desorption profiles obtained in isooctane at 80 °C suggested that the bidentate adsorbate with the most densely packed alkyl chains, **R3ArDT**, was significantly more stable than the other SAMs, producing the following relative order for thermal stability for the dithiolate SAMs: **R3ArDT** > **R2ArDT** > **R1ArDT**.



INTRODUCTION

Surface modification via the adsorption of organic molecules on metal substrates to form self-assembled monolayers (SAMs) has been explored and extensively developed for a number of novel practical applications,^{1–4} including intervening films for mechanical interfacial interactions such as friction,^{3–6} lubrication, and adhesion,^{7–9} and also for chemical and bio-related applications (e.g., sensing, molecular recognition, and conjugation of biomolecules).^{10–14} SAMs derived from organosulfur compounds on gold substrates have been particularly useful because of their convenient preparation by chemisorption of thiol adsorbates from dilute solutions. In addition, the resultant films provide well-defined structures and predictable interfacial properties.¹⁵ These thin film properties correlate to the molecular structures of the adsorbates and thus can be controlled by judicious design.¹⁵

The highly ordered and well-defined SAMs obtained from *n*-alkanethiols of suitable chain lengths (≥ 10 carbon atoms) serve as excellent models and as good starting points for the investigation of structure–property relationships. The modification of this linear structure by the addition of components differing in archetype can disturb the lateral interactions with respect to structural conformation, ordering, and stability for the associated SAM films due to changes in physical

dimensions, polarity, and chemical reactivity associated with the introduced components.¹⁶ Further, recent reports have examined a number of headgroup designs utilizing multiple surface bonds to enhance thin-film stability.^{14,15,17–24} Although SAMs derived from a variety of adsorbate molecules having substantially different chemical architectures have been investigated, there is limited information in the literature regarding the commensurability between multidentate headgroups and the long alkyl chain tailgroups typically associated with such assemblies.²⁴

Multiple attachments for an adsorbate onto the surface enhance the stability of the resultant film via the entropy-driven chelate effect;^{24–29} however, in many cases, the mismatch between the chelating headgroups and tailgroups decreases the degree of conformational order and packing density of the resulting molecular assembly.^{20,29,30} For example, the adsorption of multidentate tripodal headgroups typically with single-chain tailgroups connecting to a single point at a quaternary atom generates loosely packed and poorly ordered SAMs on gold.^{20,31} These properties arise from the relatively large

Received: January 12, 2017

Revised: March 30, 2017

Published: April 6, 2017

dimensions of the adsorbate headgroups as compared to the tailgroups, which give rise to an increase in the lateral space between molecular chains, leading consequently to a decrease in van der Waals interactions between the chains. Thus, the importance of balancing these counterparts (headgroups and tailgroups) to produce a stable SAM is considerable and should be recognized as one of the key parameters to obtain densely packed and/or highly ordered SAMs derived from multidentate adsorbates. A strategy for preparing such SAMs is based upon minimizing the lateral space and increasing the interchain interactions. For example, adsorbates can be designed to possess an additional molecular chain or branched chain to fill any void volume, thereby increasing chain-to-chain interactions and enhancing the conformational order of the monolayers. However, components such as bulky steric side groups and branched chains with an inappropriate number of branches can cause low molecular packing densities and conformationally disordered SAMs. Thus, the optimal numbers of molecular chains associated with a set of multidentate headgroups required to form a well-ordered and stable monolayer must be determined for a particular adsorbate design.

Earlier research by our group addressed such concerns in a related spiroalkane system by characterizing SAMs generated from a series of systematically designed adsorbates having bi- and tridentate chelating headgroups with one or two alkyl chains (or a methyl group and an alkyl chain) connected to a central carbon atom: 2-alkyl-2-methylpropane-1,3-dithiols (1),³⁰ 2-monoalkylpropane-1,3-dithiols (2),^{29,31} 2,2-dialkylpropanedithiols (3),^{25,29,31} and 1,1,1-tris(mercaptomethyl)alkanes (4)²⁰ as illustrated in Figure 1 (compounds 1–4).

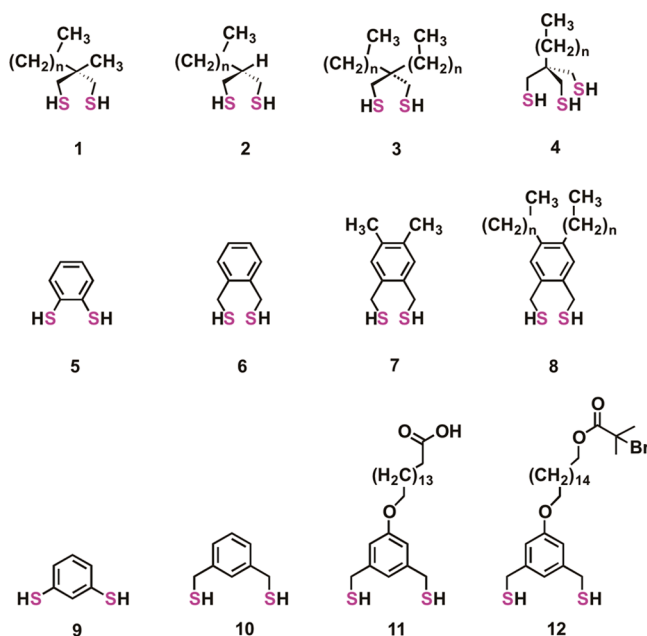


Figure 1. Spiroalkane-based and aromatic multidentate adsorbates examined in previous reports.^{17,19,24–27,29–33}

For each study, an alkanethiolate SAM (CnSH) was used as a reference system. The degree of conformational order and packing density of the alkyl chains of the SAMs generated from these adsorbates in general decreased as a function of sulfur-to-alkyl ratio: CnSH > 3 > 2 > 1 > 4.^{20,25,29,30} The lower density of the alkyl chains in the films derived from 1 as compared to

those derived from 2 can be rationalized by the steric influence of the methyl group near the quaternary carbon center.³⁰

Separately, we have also studied a number of multidentate aromatic adsorbates (see Figure 1; compounds 5–12).^{17,19,32,33} One of the advantages of aromatic-based adsorbates in terms of molecular design and synthesis is that adjusting the positioning of the functional groups on the aromatic rings can generally be accomplished in relatively few synthetic steps, affording the desired interfacial properties for the targeted monolayer film. Furthermore, aromatic-based adsorbates are advantageous due to their structural rigidity and properties associated with π -conjugation.^{34–36} Notably, we characterized and examined the thermal stability of SAMs derived from bidentate aromatic dithiols possessing two tailgroups.^{26,32} The resulting monolayer films generated from these adsorbates exhibited the same interfacial properties when compared to a densely packed analogue prepared from an *n*-alkanethiol (CnSH); however, thermal stability studies showed that the bidentate aromatic SAMs were more stable than the monodentate alkane SAMs.³² The thermal stability of the former SAMs can be rationalized by not only the chelate effect^{24–33} but also the additional π - π interactions between aromatic rings that reinforce the chain assembly interactions.^{37–39}

Building upon our prior work, we hereby designed and synthesized a new series of bidentate aromatic adsorbates having thiol-to-alkyl chain ratios ranging from 2:1 to 2:3. The molecules are composed of a benzene ring serving as the interconnecting unit between the 1,3-propanedithiol headgroup and the mono-, di-, and trisubstituted alkoxy chains at the 4-, 3,5-, and 3,4,5- positions, respectively, on the aromatic ring, as shown in Figure 2. Of particular interest are our observations

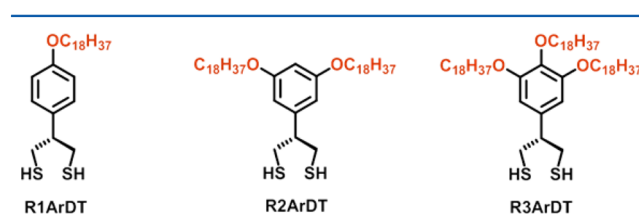


Figure 2. Structures of 2-phenylpropane-1,3-dithiols having single (R1ArDT), double (R2ArDT), and triple (R3ArDT) chains.

regarding the differences in the commensurability between the bidentate headgroups and the numbers of hydrocarbon chain tailgroups and the resulting influence that these differences have upon structural conformation, molecular packing density, and the thermal stability for the associated monolayers. These results should help contribute to the development of fundamental guidelines for adsorbate molecular design and the anticipated structure–property relationships within monolayer films based on aromatic multidentate adsorbates.

EXPERIMENTAL SECTION

Detailed information regarding materials, synthetic procedures, and instrumental methods used to conduct the research outlined in this report are provided in the Supporting Information, including ¹H and ¹³C NMR spectra for all the new adsorbates (see Figures S1–S6).

RESULTS AND DISCUSSION

Developing well-ordered SAMs from multidentate adsorbates requires a solvent system that enables effective surface bonding of the adsorbates and efficient film formation but will not

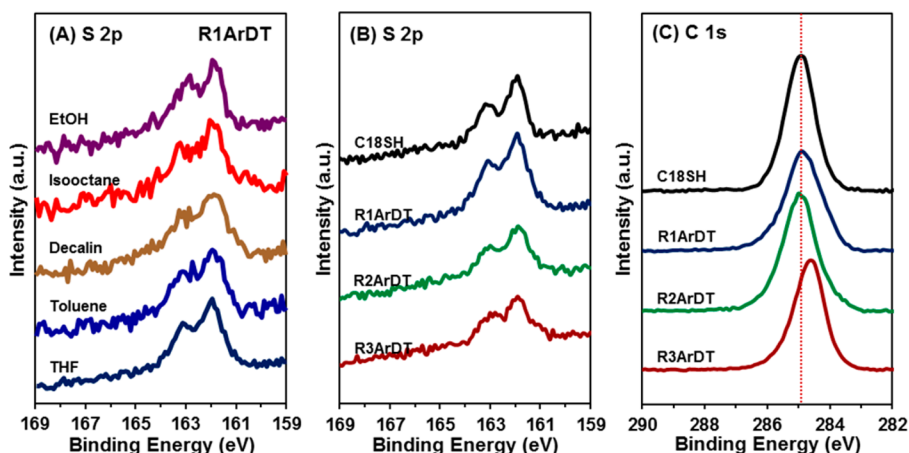


Figure 3. XPS spectra of the (A) S 2p region for the monolayers derived from R1ArDT in various solvents, (B) S 2p region, and (C) C 1s region for the monolayers derived from C18SH, R1ArDT, R2ArDT, and R3ArDT using THF as the deposition solvent.

intercalate within the adsorbate chains and alter the characteristics of the SAM. Therefore, we first sought to identify an optimal solvent for the generation of the SAMs derived from R1ArDT, R2ArDT, and R3ArDT. We used X-ray photoelectron spectroscopy (XPS) to analyze the effectiveness of a series of test solvents, as described in the next section. Once an appropriate solvent system was determined for these new adsorbates, the balance of our experimental work was conducted with the dithiolate SAMs formed in that solvent. The properties of the resultant monolayer films derived from these adsorbates were characterized and compared to those generated from octadecanethiol (C18SH) generated in ethanol. SAMs on gold derived from C18SH serve as both an internal standard, having the same chain length as those in the alkoxy substituents, and a model well-packed conformationally ordered monolayer.

Effect of Solvent on SAM Film Formation for Bidentate Aromatic Adsorbates. To investigate the optimum properties of SAMs generated from our new bidentate adsorbates, thermal stability in particular, the degree to which the sulfur atoms bind to the surface becomes a key concern.^{27,40} Structural studies of SAMs generated from normal alkanethiols by electron diffraction and low-energy electron diffraction have shown that the lattice spacing between sulfur headgroups binding on the Au(111) surface is approximately 5 Å.^{41,42} On the basis of the structural composition of the “spiroalkanedithiol” headgroup (see Figure 1), our group has previously noted that the distance between the two sulfur atoms in these branched adsorbates fails to accommodate the binding of both sulfurs on the 3-fold hollow sites of the Au(111) surface.²² Nevertheless, analysis by XPS of SAMs generated from spiroalkanedithiol adsorbates revealed that both sulfur atoms are able to bind fully to the surface without generating unbound thiols or intermolecular disulfide formation.^{25,29,30} Therefore, given the structural relationship of the spiroalkanedithiols to our new bidentate aromatic adsorbates, we anticipated that the sulfur atoms of these new adsorbates should also bind fully to the surface of gold. For SAMs studies, the choice of solvent in which the monolayers are developed is crucial for generating high quality thin films.^{43–45} Thus, to investigate the structural properties of the bidentate adsorbates, we evaluated the effect of a variety of solvents on the formation of a fully bound dithiolate film on gold (nonpolar aprotic solvents: isooctane, decalin, and toluene; polar aprotic solvent:

THF; polar protic solvent: EtOH).^{25,29} Further, we used R1ArDT as a model adsorbate to study the effect of the solvents due to its low cost and ease of preparation compared to the other multidentate adsorbates. Analysis by XPS of the S 2p region of the R1ArDT SAMs shows the presence of predominantly gold-bound sulfur thiolates, which are known to produce a doublet with binding energies of 162.0 and 163.2 eV (Figure 3 A).^{46,47} Importantly, the peak fitting results presented in Figure S7 and Table S1 indicate that the R1ArDT SAM prepared in THF exhibits 97.9% bound thiol, which is higher than that found when using the other solvent systems. In addition, there are no peaks associated with unbound or oxidized sulfur species at binding energies of ~164–165 eV¹⁶ or 166–168 eV,¹⁷ respectively.^{46,49} Consequently, we used THF as our solvent for the preparation of SAMs generated from this new series of adsorbates for further characterization and evaluation. The XPS spectra of the S 2p region in Figure 3B provides evidence that the sulfur atoms are fully bound on the gold surface for monolayers obtained from R2ArDT and R3ArDT.

Packing Density of the Films. Analyses by XPS using the S 2p signal of the thiolate headgroups can also be used to compare the relative packing characteristics of similarly structured SAMs.⁴⁶ More specifically, our previous studies reported the use of the sulfur-to-gold (S/Au) ratio to examine quantitatively the adsorbate packing density of thiolate films.¹⁹ To use this method to compare the relative presence of C18SH on a gold surface versus monolayers derived from the dithiolate adsorbates, it was necessary to divide the atomic concentration of sulfur for the SAMs formed from the bidentate adsorbates by a factor of 2. For our analysis, we utilized the integrated areas under the spectral peaks for the photoelectron emissions for the Au 4f and S 2p orbitals for the SAMs generated from C18SH and the bidentate adsorbates as presented in Table 1 (three independent samples each). A review of the data reveals that as the number of hydrocarbon chains attached to the aromatic framework increases, the S/Au ratios of the SAMs generated from the bidentate adsorbates decrease. These results reflect the larger space on the underlying gold surface required for the adsorbed molecules as their overall steric bulk increases, yielding the following order for surface area per adsorbate: R3ArDT > R2ArDT > R1ArDT > C18SH. The *molecular packing densities* of the R1ArDT, R2ArDT, and R3ArDT monolayers yield values of 59%, 49%, and 44% per unit area,

Table 1. Adsorbate and Alkyl Chain Packing Densities for the SAMs Derived from R1ArDT, R2ArDT, and R3ArDT Relative to C18SH Calculated Using the S/Au Ratio

adsorbate	S/Au			relative adsorbate density ^a (%)	relative alkyl chain density (%)
	sample 1	sample 2	sample 3		
C18SH	0.052	0.054	0.051	100	100
R1ArDT	0.066	0.066	0.056	59 ± 4.2	59 ± 4.2 ^b
R2ArDT	0.050	0.052	0.052	49 ± 1.7	98 ± 3.4 ^c
R3ArDT	0.046	0.050	0.042	44 ± 2.0	132 ± 6.0 ^d

^aTo compare the adsorbate densities, the S/Au ratios of SAMs derived from the dithiolates were divided by a factor of 2 compared to the SAM derived from C18SH. ^bTo derive these chain densities, the adsorbate densities were multiplied by a factor of 1 compared to the SAM derived from C18SH. ^cTo derive these chain densities, the adsorbate densities were multiplied by a factor of 2 compared to the SAM derived from C18SH. ^dTo derive these chain densities, the adsorbate densities were multiplied by a factor of 3 compared to the SAM derived from C18SH.

respectively, relative to 100% for the C18SH monolayer. On the other hand, the *alkyl chain densities* for the new SAMs decrease as follows: R3ArDT > R2ArDT > R1ArDT, reflecting the corresponding values of 132%, 98%, and 59%, respectively, due to the ratio of alkoxy chains per adsorbate. These trends are unsurprising and can be rationalized based on the chain-to-headgroup ratios and the void space that would be present in a normal alkanethiolate chain assembly if the chains did not tilt in response to van der Waals attractions between alkyl chains (i.e., if the chains aligned parallel to the surface normal).

Ellipsometric Thickness Measurements. Measurement of the ellipsometric thicknesses not only allows an estimation of the thickness of a fully developed monolayer film, but also can be used to monitor the progress of film growth over time.^{43,51} The thicknesses of monolayer films generated from our bidentate adsorbates were measured after 72 h of exposure of the gold slides in the deposition solutions. Little change or no difference in the thickness values were observed for longer immersion times. The longer equilibration time required for complete monolayer formation from these monolayer adsorbates as compared to that for C18SH (typically 24 h) can be attributed to the slower diffusion of the bidentate adsorbates on the surface of gold due, not only to their bidentate nature, but also to the steric and conformational constraints of these adsorbates.²⁵ In addition, prior reports by our group suggest that the mismatch between the bidentate headgroup and the Au(111) lattice might give rise to the need for a longer equilibration time; for SAMs to be fully formed, reconstruction of the underlying gold surface might be required to generate an environment for the successful binding of the headgroups.²⁵

In the present analysis, we first started by considering monolayers generated from the aromatic dithiols using a qualitative interpretation of the ellipsometric thicknesses relative to the chain orientation and conformational order. The large dimensions of the chelating dithiol headgroups and the alignment of the rigid aromatic rings can disturb the molecular packing density by enhancing the space between neighboring adsorbates. The increasing space between chains therefore causes the chains to tilt toward adjacent chains in order to diminish free volume and to optimize chain–chain van der Waals interactions. These adjustments to the structural

alignments of the adsorbates can lead to improvements in the conformational ordering of the alkyl chains in the thin-film assembly. On the other hand, if these chain–chain interactions are insufficient to stabilize the system (e.g., minimizing the conformational mobility of the chains by achieving low energy structural alignments), they might give rise to disruptions of the conformational order of the long hydrocarbon chains (e.g., gauche conformations in the alkyl chains and the development of monolayer film defects).^{37–39,52}

The data in Table 2 show a comparison of the experimentally determined thicknesses and the calculated thicknesses

Table 2. Calculated Thicknesses and Measured Thicknesses for SAMs Generated from C18SH, R1ArDT, R2ArDT, and R3ArDT

adsorbate	calculated thickness (Å)	ellipsometric thickness ^a (Å)
C18SH	22	21.2 ± 0.2
R1ArDT	31	18.5 ± 0.6
R2ArDT	30	23.1 ± 0.3
R3ArDT	30–31	29.0 ± 0.6

^aValues reflect the average and standard deviation derived from 18 data points.

estimated using molecular models assuming that the long alkoxy chains fully adopt *trans* conformations and tilt ~30° from the surface normal, which is based on the tilt angle of the alkyl chains in model alkanethiol SAMs on gold,⁴ and that the orientation of the phenyl ring is perpendicular to the surface normal, as shown in Figure S8. The data in Table 2 show two apparent features worth noting. First, the ellipsometric thicknesses of the R1ArDT and R2ArDT monolayers are notably less than the theoretical values, while the ellipsometric thickness of the R3ArDT monolayer is approximately the same as the thickness obtained from the molecular model.⁶¹ Second, the thicknesses of the SAMs as measured by ellipsometry increase with increasing numbers of branched chains. With the molecular structures in Figure 4, the potential void volume above the phenyl rings decreases going from R1ArDT > R2ArDT > R3ArDT. As noted above, the low measured thicknesses of the R1ArDT and R2ArDT monolayers can be rationalized by an increase in chain tilt and/or chain deformation that occurs when the chains adopt low-energy structural alignments/conformations.

On the other hand, the thickness of the R3ArDT SAM measured by ellipsometry is close to that obtained from the model, which suggests that the long alkoxy chains in the R3ArDT monolayer are likely tilted less with respect to the surface normal as compared to those in any of the other monolayers in this series. From the measured ellipsometric thicknesses, the relative chain tilt of the SAMs generated from these new adsorbates can be qualitatively estimated as follows: R1ArDT > R2ArDT > R3ArDT, while the trend in the conformational order of the alkyl chains would logically exhibit the reverse trend from the relative chain tilt. We collected additional characterization data to define more clearly how these SAMs were organized and how to rationalize the observed trends in the ellipsometric thicknesses.

Conformational Analysis by PM-IRRAS. The specific technique of polarization modulation infrared reflection–absorption spectroscopy (PM-IRRAS) can be used to evaluate the relative surface orientation and conformational order of the adsorbate chains of organic thin films.^{54,55} Figure 5 shows the

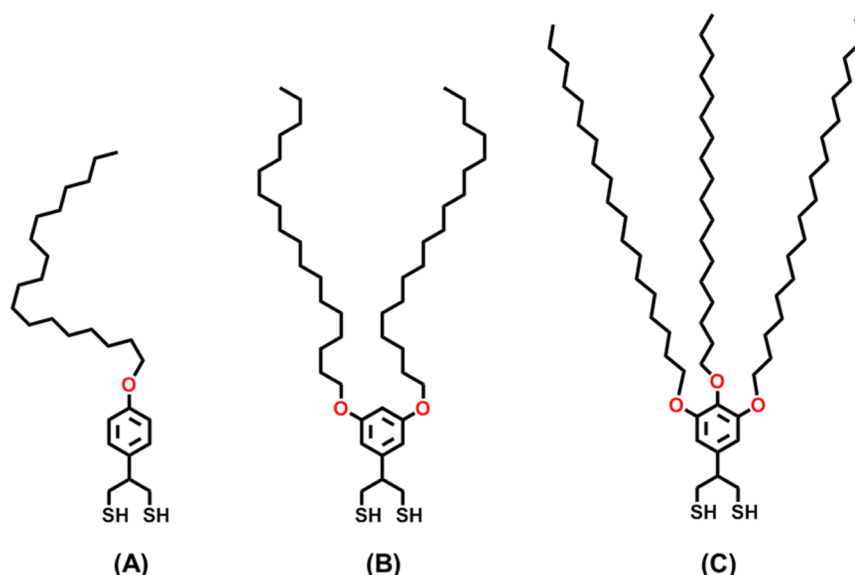


Figure 4. Anticipated structural representations of (A) R1ArDT, (B) R2ArDT, and (C) R3ArDT based on results from the ellipsometric thickness measurements.

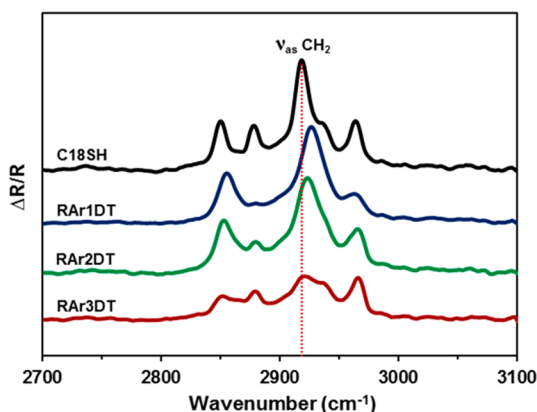


Figure 5. PM-IRRAS spectra showing the C–H stretching region for the monolayer films derived from C18SH, R1ArDT, R2ArDT, and R3ArDT.

C–H stretching region of the surface infrared spectra of SAMs derived from C18SH and the new bidentate aromatic dithiol adsorbates. The position of the antisymmetric methylene stretching ($\nu_{\text{as}}^{\text{CH}_2}$) band for the C18SH SAM is observed at 2918 cm^{-1} , consistent with a crystalline-like alkyl chain assembly for this monolayer film.⁵³ Any shift of the $\nu_{\text{as}}^{\text{CH}_2}$ band to a higher frequency than 2918 cm^{-1} indicates a less conformationally ordered SAM (i.e., lower crystallinity and an increasing abundance of gauche conformations along the alkoxy chains).⁵⁴

For SAMs derived from the new bidentate adsorbates, R1ArDT, R2ArDT, and R3ArDT, the position of the $\nu_{\text{as}}^{\text{CH}_2}$ band shifts to higher wavenumbers, ~ 2925 , 2923 , and 2920 cm^{-1} , respectively. The two former SAMs represent substantial shifts of the $\nu_{\text{as}}^{\text{CH}_2}$ band, indicating that their chains are more liquid-like when compared to those of the latter SAM, where the $\nu_{\text{as}}^{\text{CH}_2}$ band shifted to only slightly higher wavenumber ($\Delta 2\text{ cm}^{-1}$) relative to that of the crystalline-like conformational structure of the C18SH monolayer film. The lower crystallinity of the R3ArDT monolayer compared to the C18SH monolayer can be attributed to the structurally constrained hydrocarbon

chains in the R3ArDT SAMs, which can plausibly lead to partial disorder in the alignment of the chains. Additionally, what is apparent from these data is that the loss of crystallinity aligns with the reduction in the number of alkyl chains. Based on the peak position of $\nu_{\text{as}}^{\text{CH}_2}$ band, the degree of conformational order for these monolayers decreases in the following order: C18SH > R3ArDT > R2ArDT > R1ArDT.

Another interesting feature of the IR spectra in the C–H stretching region in Figure 5 is the presence of the broad bands of the Fermi resonance of the symmetric methyl stretching ($\nu_{\text{s}}^{\text{CH}_3}$ FR) appearing at $\sim 2935\text{ cm}^{-1}$ in the spectra of the C18SH and R3ArDT monolayers. On the other hand, in the case of the R1ArDT and R2ArDT films, the contribution of the Fermi resonance bands are less significant and fully overlap with the $\nu_{\text{as}}^{\text{CH}_2}$ bands. It has been reported that the observation of a predominant Fermi resonance band is indicative of strong chain–chain interactions.^{57,58} Therefore, the results indicate that strong chain assembly interactions exert a greater impact on the monolayer films derived from the C18SH and R3ArDT monolayers, while having less impact on the R1ArDT and R2ArDT monolayers.

Taking all IR results together, we discovered that the conformational order and the interplay of chain–chain interactions for the monolayers derived from these bidentate adsorbates increase as the numbers of branched chains increase. This correlation can be rationalized in terms of the chain packing density (namely, chain-to-headgroup ratios) and commensurability between the dithiolate headgroup and branched chain tailgroups. For example, in the case of the R3ArDT monolayer, the cross-sectional area of the triple-chained hydrocarbon branches is larger than the area occupied by the dithiolate headgroup on the gold surface, giving rise to a film with comparatively low molecular packing density on the surface. However, the presence of the well-ordered conformation of the hydrocarbon chains is due to the attractive chain–chain interactions between densely packed alkoxy chains in the film, a model that is supported by the collective PM-IRRAS and XPS data.

On the other hand, for the R1ArDT monolayer, the aromatic dithiolate headgroup is a mismatch to the single-chained

Table 3. Advancing (θ_a) and Receding (θ_r) Contact Angles and Hysteresis ($\Delta\theta = \theta_a - \theta_r$) for Hexadecane, Water, and Decalin on SAMs Derived from C18SH, R1ArDT, R2ArDT, and R3ArDT

adsorbate	water ^a			hexadecane ^a			decalin ^a		
	θ_a	θ_r	$\Delta\theta$	θ_a	θ_r	$\Delta\theta$	θ_a	θ_r	$\Delta\theta$
C18SH	114 ± 1.5	104 ± 1.0	10	50 ± 1.0	40 ± 0.5	10	54 ± 1.0	47 ± 0.5	6
R1ArDT	108 ± 0.5	98 ± 0.5	10	44 ± 0.5	34 ± 0.5	10	32 ± 0.5	26 ± 0.5	5
R2ArDT	111 ± 1.1	101 ± 0.8	10	42 ± 1.5	32 ± 1.0	10	38 ± 1.0	32 ± 1.0	6
R3ArDT	113 ± 1.1	103 ± 0.7	10	43 ± 0.5	34 ± 0.5	10	47 ± 1.1	37 ± 1.0	10

^aValues of θ_a and θ_r reflect the average and standard deviation derived from 18 data points.

tailgroup, in which the cross-sectional area of the hydrocarbon chain is smaller relative to the area occupied by the headgroup. Although the molecular packing of the R1ArDT monolayer is more dense relative to that of the R2ArDT and R3ArDT monolayers, the incommensurability between the headgroup and the single hydrocarbon chain in R1ArDT causes a loose chain packing and deformation of the long alkoxy chains due to a reduction in the chain packing assembly. For R2ArDT, the 1:1 ratio of the sulfur atoms in the headgroup to the long alkoxy chains (as is the case with C18SH) leads to a chain packing density of 98%, comparable to the densely packed C18SH monolayer. Indeed, the addition of two long alkoxy chains improves the conformational order of the R2ArDT SAM when compared to that of R1ArDT SAM; however, the film is still less conformationally ordered than the C18SH SAM. These results can be attributed to the large size of the bidentate aromatic headgroup and also the incommensurate packing between the 3,5-branched chains that perturb the molecular packing density and diminish the chain–chain interactions of the R2ArDT SAM.

Wettability of the Films. Measurement of contact angles for contacting liquids is one of the fundamental techniques to determine the structure and quality of an organic thin film.⁵⁹ The wettability data in Table 3 show that the advancing contact angles of water ($\theta_a^{\text{H}_2\text{O}}$) were 115°, 109°, 111°, and 113° for SAMs generated from C18SH, R1ArDT, R2ArDT, and R3ArDT, respectively, indicating that the interfaces formed by the new bidentate aromatic dithiols are hydrophobic. However, the contact angles of water provide less information regarding the chain orientation and conformational order of hydrophobic monolayer films when compared to those of hexadecane (HD). Hexadecane is a highly sensitive liquid for probing the interfacial hydrocarbon surfaces and identifying loosely packed SAMs, in which hexadecane wets interfacial methylene groups more than interfacial methyl groups.^{43,60}

Unexpectedly, the contact angles of hexadecane for all the monolayer surfaces derived from the new bidentate adsorbates revealed no substantial differences in the interfacial wetting (i.e., the values of θ_a^{HD} fell within a range of 42°–45°). These results are somewhat inconsistent with the model of the films developed from the ellipsometric thickness measurements and the conformational order determined by PM-IRRAS. On the basis of these results, we hypothesized that hexadecane might be intercalating into the loosely packed chains of R1ArDT and R2ArDT SAMs, filling the void space between the long alkyl chains, and giving θ_a^{HD} values comparable to the R3ArDT SAM, where the alkyl tailgroups are densely packed (*vide supra*).

To test for the possibility of intercalation, we employed decalin, a sterically bulky molecule unlikely to intercalate into the R1ArDT and R2ArDT films. The advancing contact angles of decalin (θ_a^{DEC}) for SAMs obtained from all adsorbates are

shown in Table 3. This liquid shows markedly greater wettability on the R2ArDT SAM ($\theta_a^{\text{DEC}} = 38^\circ$) and even more so on the R1ArDT SAM ($\theta_a^{\text{DEC}} = 32^\circ$) when compared to that on the densely packed R3ArDT SAM ($\theta_a^{\text{DEC}} = 47^\circ$). Notably, a reduced value of θ_a^{DEC} indicates that methylene rather than methyl groups are exposed at the interface.^{42,59} Further, the θ_a^{DEC} values for these monolayers decrease with decreasing numbers of alkyl tailgroups in the bidentate adsorbates; specifically, these data are consistent with the model of the films developed from the analyses of the ellipsometric and PM-IRRAS data (*vide supra*). Separately, comparison of the wettability of decalin on the R3ArDT SAMs with that on the C18SH SAMs suggests that the interface of the former SAM is less homogeneous than that of the latter. This inference is supported by the larger contact angle hysteresis ($\Delta\theta^{\text{decalin}}$) on the R3ArDT SAM. The increase in interfacial heterogeneity can plausibly arise from a change in the tilt angle and/or a reduction in the conformational order of the chains. Therefore, we conclude that the conformational order of the long alkoxy chains in the SAMs studied here decrease in the following order: C18SH > R3ArDT > R2ArDT > R1ArDT.

Thermal Stability of SAMs Formed from R1ArDT, R2ArDT, and R3ArDT. In previous reports of SAMs derived from spiroalkanedithiols,^{23,28–31} the enhanced thermal stability was rationalized on the basis of the chelate effect, which restricts desorption of the adsorbates (1) as intramolecular cyclic disulfides owing to ring strain effects and (2) as intermolecular disulfides, requiring the formation of dimers (bis-disulfides), trimers (tris-disulfides), or even larger heterocycles owing to the entropically disfavored loss of multiple surface bonds.³¹ As an analogous chelating headgroup, we anticipated that the bidentate aromatic headgroup of the new adsorbates would yield SAMs with thermal stability characteristics comparable to those generated from the spiroalkanedithiol adsorbates.³¹ In addition, we expected the results to lead to a better understanding of the relationship between the number of branched chains and their influence on the thermal stability of multidentate SAMs.

We investigated the thermal stability by monitoring the solution-phase desorption of SAMs generated from the new bidentate aromatic adsorbates by using ellipsometry and PM-IRRAS to track the thickness and conformational changes of each monolayer film over time.^{19,28,33} While several thermal stability studies of SAMs by our group and others have been conducted under ultrahigh vacuum (UHV) conditions that allowed for *in situ* XPS characterization of the films,^{62,63} we chose the solution-phase desorption method because it allows for a facile evaluation of changes in thickness and conformational order of multiple SAM samples using both ellipsometry and PM-IRRAS. Thus, the films were heated in isooctane at 80 °C to evaluate their thermal stability in a hydrocarbon solvent. We chose isooctane due to its bulky end groups that are

sterically hindered and thus intercalate poorly in the monolayer films. As evaluated by ellipsometry, all SAMs under investigation exhibited a two-stage desorption profile as shown in Figure 6: a fast initial desorption regime followed

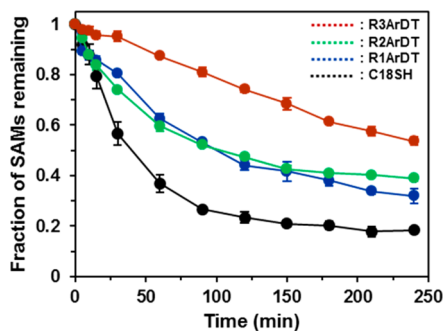


Figure 6. Desorption profiles determined by ellipsometric measurements of the monolayers derived from C18SH, R1ArDT, R2ArDT, and R3ArDT upon heating in isooctane at 80 °C. Data for three independent analyses per adsorbate are shown (i.e., 18 data collections per point); nonvisible error bars fall within the symbols.

by a substantially slower or nondesorbing regime. The desorption profiles of the monolayers generated from these adsorbates are in good agreement with the literature descriptions reported for the desorption of alkanethiolate-based SAMs on gold surfaces.^{59,60} Previous studies from other research groups and those generated by our group rationalized the two stages in the desorption profile as a consequence of the adsorbates having two distinct binding sites; at the first site, thiolate headgroups are bound weakly on gold, giving rise to an initial fast desorption process, while the second site provides a stronger binding of the thiolate headgroups where little or no desorption occurs.^{31,32,61,64}

After 90 min of heating, the fraction of adsorbate remaining decreased drastically to 27, 47, and 52% of the initial SAMs generated from C18SH, R1ArDT, and R2ArDT, respectively; and after 150 min of heating, the fractions were 24, 40, and 42%, respectively, indicating a markedly slower desorption process. Longer heating times led to little or no desorption. In contrast, monolayers generated from R3ArDT exhibited a relatively slow and linear loss of thickness, with ~54% of the SAM remaining at 240 min, whereas the remaining fractions of

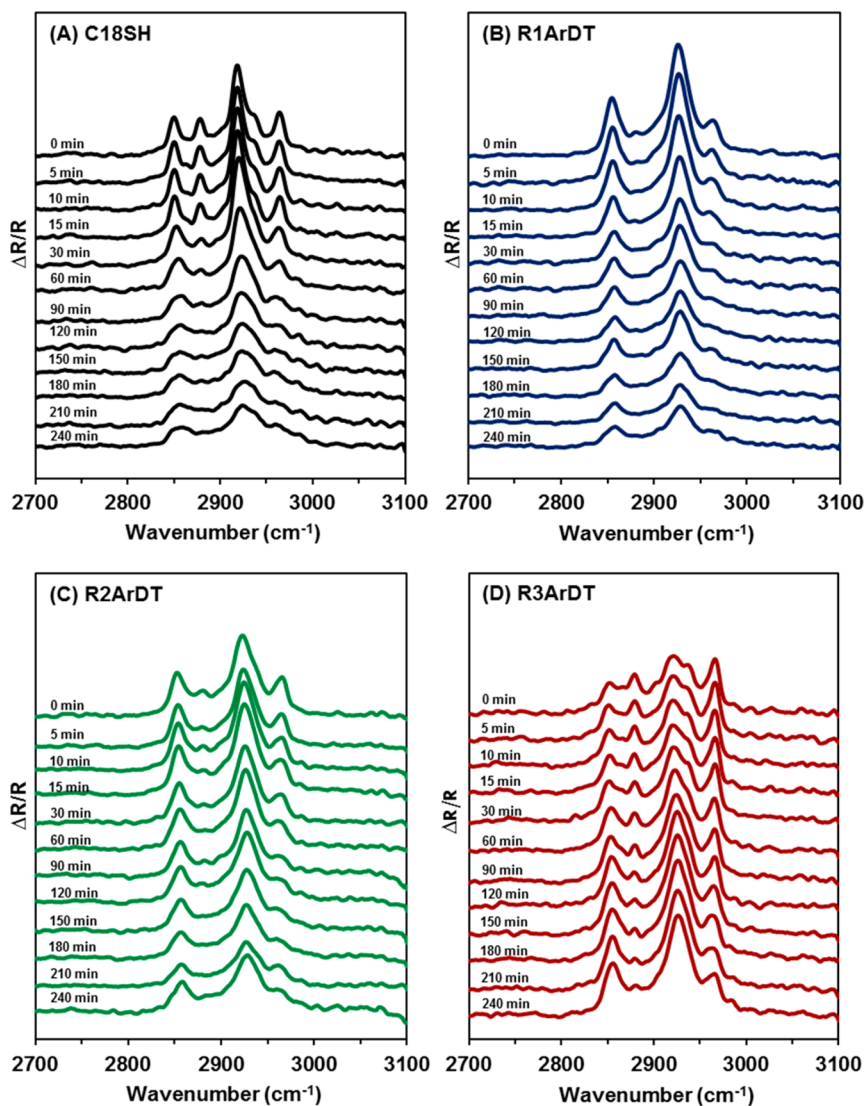


Figure 7. PM-IRRAS spectra of the C–H stretching region of the (A) C18SH, (B) R1ArDT, (C) R2ArDT, and (D) R3ArDT monolayers as a function of time under heat treatment at 80 °C in isooctane.

SAMs generated from **C18SH**, **R1ArDT**, and **R2ArDT** were ~18%, 32%, and 39%, respectively. As a whole, the desorption profiles indicate that the **R3ArDT** monolayer is more resistant to thermal desorption than the other bidentate monolayers (**R1ArDT** and **R2ArDT**), which are themselves more resistant to thermal desorption than the **C18SH** monolayer.

To provide a more quantitative analysis of the thermal stability of these monolayers, we analyzed the rates of desorption by fitting the data into two regime profiles, separately. While the rate constants in the fast-desorbing regime can be established by fitting the data with a first-order kinetic equation,⁴³ we were unable to analyze the data similarly in the slow/nondesorbing regime due to the statistically insignificant changes in ellipsometric thickness measured for the SAMs (i.e., changes in thickness of SAMs that were within ± 2 Å). Therefore, we chose to evaluate the relative thermal stabilities of these SAMs based solely on the rates of desorption in the fast-desorbing regime. The desorption data in the fast-desorbing regime were fitted to first-order kinetics according to eq 1.⁴³

$$(T_t - T_\infty)/(T_0 - T_\infty) = e^{-kt} \quad (1)$$

In this equation, T_0 is the initial thickness of the SAM, T_t is the thickness of the SAM at time t , and T_∞ is the ultimate thickness of the SAM at an infinite time span (using ~30 h). The rate constants for desorption of the monolayers were obtained at 80 °C in isooctane, and the rate constants of SAMs formed with **C18SH**, **R1ArDT**, **R2ArDT**, and **R3ArDT** were 2.37, 1.82, 1.46, and 0.42×10^{-2} (min^{-1}), respectively. A comparison of the rate constants shows that the **C18SH** monolayers desorb faster than any of the monolayers derived from the bidentate adsorbates. In addition, across the entire desorption profile, the fraction of SAM remaining derived from the bidentate adsorbates was higher than that for the SAM derived from **C18SH**. As such, the results again illustrate an enhanced thermal stability for bidentate SAMs due to the chelate effect.

With a further comparison of the rate constants, we can explore the influence of the varying numbers of branched chains upon the thermal stability of the monolayers obtained from these bidentate adsorbates. The rates of desorption increase with decreasing numbers of long alkoxy chains, indicating the key role of intramolecular chain-to-chain interactions in stabilizing monolayers.⁴³ In our new SAMs, the overall strength of the chain–chain van der Waals interactions is proportional to the number of alkyl tailgroups in the bidentate adsorbates. Consequently, we might predict a correlation between the desorption behavior and the degree of chain conformational order, considering that the most ordered conformation (implying strong van der Waals interactions) of the long alkoxy chains should afford films with the most resistance to thermal desorption.^{43,56} To explore this possible correlation, we examined *ex situ* the positions and bandwidths of the asymmetric methylene stretching band ($\nu_{\text{as}}^{\text{CH}_2}$), which is sensitive to conformational order.^{54,55,65,66} Indeed, the $\nu_{\text{as}}^{\text{CH}_2}$ values at room temperature suggest that the SAMs derived from **R3ArDT** ($\sim 2920 \text{ cm}^{-1}$) would be the more stable than those derived from **R1ArDT** ($\sim 2925 \text{ cm}^{-1}$) and **R2ArDT** ($\sim 2923 \text{ cm}^{-1}$), which is consistent with our observations (see Figure 7). On the other hand, the SAM derived from **C18SH** ($\nu_{\text{as}}^{\text{CH}_2} = \sim 2918 \text{ cm}^{-1}$) is even more conformationally ordered than that derived from **R3ArDT** ($\nu_{\text{as}}^{\text{CH}_2} = \sim 2920 \text{ cm}^{-1}$), but it is markedly less thermally stable. This apparent discrepancy is

however, further evidence of the overwhelming impact on stability afforded by the chelate effect.

We also examined the PM-IRRAS spectra in the C–H stretching region of all monolayers as a function of time at 80 °C in isooctane (see Figure 7). In general, the PM-IRRAS spectral profiles for the SAMs derived from **C18SH**, **R1ArDT**, and **R2ArDT** are similar, with the intensity of the $\nu_{\text{as}}^{\text{CH}_2}$ bands gradually decreasing and their band position shifting to higher frequency with increasing heating time. The SAM derived from **R3ArDT** provides contrast, with the intensity of the $\nu_{\text{as}}^{\text{CH}_2}$ bands gradually increasing and its band position shifting to higher frequency with increasing heating time. The shifts in the $\nu_{\text{as}}^{\text{CH}_2}$ band positions to higher frequency during the desorption process for all of the SAMs indicate a transition to relatively greater conformational disorder^{65,66} associated with an accumulation of gauche defects.^{66,67} Further, the decrease in the $\nu_{\text{as}}^{\text{CH}_2}$ band intensity for the **C18SH**, **R1ArDT**, and **R2ArDT** SAMs is consistent with the progressive desorption of these films from the surface.

The interpretation of the spectral trends for the **R3ArDT** SAM is more complicated. As mentioned above, the **R3ArDT** SAM is less tilted on the surfaces than the other SAMs. Hence, the $\nu_{\text{as}}^{\text{CH}_2}$ is likely oriented more parallel to the surface of gold, which would plausibly lead to the low intensity observed for this band ($\sim 2920 \text{ cm}^{-1}$) at room temperature. However, the subsequent removal of adsorbates upon heat treatment causes the remaining **R3ArDT** molecules to reorient on the surface, increasing the tilt angle of molecules from the surface normal; consequently, the $\nu_{\text{as}}^{\text{CH}_2}$ becomes oriented more perpendicular to the surface of gold, thereby leading to the observed increase in intensity and wavenumber of the $\nu_{\text{as}}^{\text{CH}_2}$ band for these SAMs upon thermal desorption.^{66,68,69}

As a whole, we can conclude that the chelate effect for these bidentate adsorbates provides the greatest contribution to monolayer stability. Although the SAM derived from **R1ArDT** is more loosely packed and disordered than that derived from **C18SH**, the thermal stability of the chelating SAM is clearly greater than the **C18SH** SAM. However, in the case of the comparison between the monolayers derived from the bidentate adsorbates themselves, the difference in thermal stability arises from the magnitude of the chain–chain interactions, as generated by both inter- and intramolecular contributions. To summarize, the thermal stability of these monolayers increases according to the following trend: **C18SH** < **R1ArDT** < **R2ArDT** < **R3ArDT**.

CONCLUSIONS

We investigated the SAMs derived from a new series of aromatic bidentate thiols having the same bidentate headgroup but different numbers of alkyl tailgroups: **R1ArDT**, **R2ArDT**, and **R3ArDT**. All three dithiolate adsorbates bind to the surface of gold with complete binding of both sulfur headgroups. Structural characterization and investigation of thermal stability of the SAMs derived from these adsorbates reveal the significant influence of the numbers of branched chains on the degree of conformational order and stability of the monolayers. An increase in the numbers of alkyl tailgroups leads to at least three important outcomes: (1) an increase in interchain van der Waals interactions, (2) an increase in the degree of conformational order of the long alkoxy chains, and (3) an increase in the thermal stability of the monolayer. The greatest impact on thermal stability is, however, the chelate effect afforded by bidentate nature of the aromatic dithiol

adsorbates. Consequently, the thermal stability of the monolayers examined in this study increases according to the following trend: C18SH < R1ArDT < R2ArDT < R3ArDT.

■ ASSOCIATED CONTENT

📄 Supporting Information

The Supporting Information is available free of charge on the ACS Publications website at DOI: 10.1021/acs.langmuir.7b00088.

Descriptions of the materials and synthetic procedures used for preparing the 2-phenylpropane-1,3-dithiol derivatives, R1ArDT, R2ArDT, and R3ArDT, along with ¹H and ¹³C NMR and the instrumental procedures used to conduct this research (PDF)

■ AUTHOR INFORMATION

Corresponding Author

*E-mail: trlee@uh.edu (T.R.L.).

ORCID

T. Randall Lee: 0000-0001-9584-8861

Notes

The authors declare no competing financial interest.

■ ACKNOWLEDGMENTS

The National Science Foundation (CHE-1411265), the Robert A. Welch Foundation (E-1320), and the Texas Center for Superconductivity at the University of Houston provided generous support for this research.

■ REFERENCES

- (1) Love, J. C.; Estroff, L. A.; Kriebel, J. K.; Nuzzo, R. G.; Whitesides, G. M. Self-Assembled Monolayers of Thiolates on Metals as a Form of Nanotechnology. *Chem. Rev.* **2005**, *105*, 1103–1169.
- (2) Osaka, T. Creation of Highly Functional Thin Films Using Electrochemical Nanotechnology. *Chem. Rec.* **2004**, *4*, 346–362.
- (3) Carpick, R. W.; Salmeron, M. Scratching the Surface: Fundamental Investigations of Tribology with Atomic Force Microscopy. *Chem. Rev.* **1997**, *97*, 1163–1194.
- (4) Vericat, C.; Vela, M. E.; Benitez, G.; Carro, P.; Salvarezza, R. C. Self-Assembled Monolayers of Thiols and Dithiols on Gold: New Challenges for a Well-Known System. *Chem. Soc. Rev.* **2010**, *39*, 1805–1834.
- (5) Nakano, M.; Ishida, T.; Sano, H.; Sugimura, H.; Miyake, K.; Ando, Y.; Sasaki, S. Tribological Properties of Self-Assembled Monolayers Covalently Bonded to Si. *Appl. Surf. Sci.* **2008**, *255*, 3040–3045.
- (6) Cho, W. K.; Park, S. J.; Jon, S.; Choi, I. S. Water-Repellent Coating: Formation of Polymeric Self-Assembled Monolayers on Nanostructured Surfaces. *Nanotechnology* **2007**, *18*, 395602.
- (7) Bhushan, B.; Kasai, T.; Kulik, G.; Barbieri, L.; Hoffmann, P. AFM Study of Perfluoroalkylsilane and Alkylsilane Self-Assembled Monolayers for Anti-stiction in MEMS/NEMS. *Ultramicroscopy* **2005**, *105*, 176–188.
- (8) Quon, R. A.; Ulman, A.; Vanderlick, T. K. Use of the Surface Forces Apparatus to Directly Measure the Influence of Self-Assembled Monolayers on the Adhesion and Deformation of Rough Solids. *Langmuir* **2000**, *16*, 3797–3802.
- (9) Liu, H.; Bhushan, B. Investigation of Nanotribological Properties of Self-Assembled Monolayers with Alkyl and Biphenyl Spacer Chains. *Ultramicroscopy* **2002**, *91*, 185–202.
- (10) Andersson, O.; Nikkinen, H.; Kanmert, D.; Enander, K. A Multiple-Ligand Approach to Extending the Dynamic Range of Analyte Quantification in Protein Microarrays. *Biosens. Bioelectron.* **2009**, *24*, 2458–2464.
- (11) Chaki, N. K.; Vijayamohan, K. Self-Assembled Monolayers as a Tunable Platform for Biosensor Applications. *Biosens. Bioelectron.* **2002**, *17*, 1–12.
- (12) Im, H. S.; Shao, H.; Park, Y. I.; Peterson, V. M.; Castro, C. M.; Weissleder, R.; Lee, H. H. Label-Free Detection and Molecular Profiling of Exosomes with a Nano-Plasmonic Sensor. *Nat. Biotechnol.* **2014**, *32*, 490–495.
- (13) Kubackova, J.; Fabriciova, G.; Miskovsky, P.; Jancura, D.; Sanchez-Cortes, S. Sensitive Surface-Enhanced Raman Spectroscopy (SERS) Detection of Organochlorine Pesticides by Alkyl Dithiol-Functionalized Metal Nanoparticles-Induced Plasmonic Hot Spots. *Anal. Chem.* **2015**, *87*, 663–669.
- (14) Park, C. S.; Lee, H. J.; Jamison, A. C.; Lee, T. R. Robust Maleimide-Functionalized Gold Surfaces and Nanoparticles Generated Using Custom-Designed Bidentate Adsorbates. *Langmuir* **2016**, *32*, 7306–7315.
- (15) Lee, H. J.; Jamison, A. C.; Lee, T. R. Two Are Better than One: Bidentate Adsorbates Offer Precise Control of Interfacial Composition and Properties. *Chem. Mater.* **2016**, *28*, 5356–5364.
- (16) Schreiber, F. Structure and Growth of Self-Assembling Monolayers. *Prog. Surf. Sci.* **2000**, *65*, 151–256.
- (17) Chinwangso, P.; Jamison, A. C.; Lee, T. R. Multidentate Adsorbates for Self-Assembled Monolayer Films. *Acc. Chem. Res.* **2011**, *44*, 511–519.
- (18) Singhana, B.; Rittikulsittichai, S.; Lee, T. R. Tridentate Adsorbates with Cyclohexyl Headgroups Assembled on Gold. *Langmuir* **2013**, *29*, 561–569.
- (19) Park, C. S.; Lee, H. J.; Jamison, A. C.; Lee, T. R. Robust Thick Polymer Brushes Grafted from Gold Surfaces Using Bidentate Thiol-Based Atom-Transfer Radical Polymerization Initiators. *ACS Appl. Mater. Interfaces* **2016**, *8*, 5586–5594.
- (20) Park, J.-S.; Vo, A. N.; Barriet, D.; Shon, Y.-S.; Lee, T. R. Systematic Control of the Packing Density of Self-Assembled Monolayers Using Bidentate and Tridentate Chelating Alkanethiols. *Langmuir* **2005**, *21*, 2902–2911.
- (21) Zhao, Y.; Pérez-Segarra, W.; Shi, Q.; Wei, A. Dithiocarbamate Assembly on Gold. *J. Am. Chem. Soc.* **2005**, *127*, 7328–7329.
- (22) Miller, M. S.; San Juan, R. R.; Ferrato, M.-A.; Carmichael, T. B. The Unusual Self-Organization of Dialkylidithiophosphinic Acid Self-Assembled Monolayer on Ultrasoft Gold. *J. Am. Chem. Soc.* **2014**, *136*, 4212–4222.
- (23) Miller, M. S.; San Juan, R. R.; Ferrato, M.-A.; Carmichael, T. B. New Dialkylidithiophosphinic Acid Self-Assembled Monolayer (SAMs): Influence of Gold Substrate Morphology on Adsorbate Binding and SAM Structure. *Langmuir* **2011**, *27*, 10019–10026.
- (24) Bruno, G.; Babudri, F.; Operamolla, A.; Bianco, G. V.; Losurdo, M.; Giangregorio, M. M.; Omar, O. H.; Mavelli, F.; Farinola, G. M.; Capezzuto, P.; Naso, F. Tailoring Density and Optical and Thermal Behavior of Gold Surfaces and Nanoparticles Exploiting Aromatic Dithiols. *Langmuir* **2010**, *26*, 8430–8440.
- (25) Shon, Y.-S.; Lee, T. R. Chelating Self-Assembled Monolayers on Gold Generated from Spiroalkanedithiols. *Langmuir* **1999**, *15*, 1136–1140.
- (26) Garg, N.; Lee, T. R. Self-Assembled Monolayers Based on Chelating Aromatic Dithiols on Gold. *Langmuir* **1998**, *14*, 3815–3819.
- (27) Srisombat, L.-o.; Zhang, S.; Lee, T. R. Thermal Stability of Mono-, Bis-, and Tris-Chelating Alkanethiol Films Assembled on Gold Nanoparticles and Evaporated “Flat” Gold. *Langmuir* **2010**, *26*, 41–46.
- (28) Lee, H. J.; Jamison, A. C.; Lee, T. R. Entropy-Driven Conformational Control of α,ω -Difunctional Bidentate-Dithiol Azo-Based Adsorbates Enables the Fabrication of Thermally Stable Surface-Grafted Polymer Films. *ACS Appl. Mater. Interfaces* **2016**, *8*, 15691–15699.
- (29) Shon, Y.-S.; Colorado, R., Jr.; Williams, C. T.; Bain, C. D.; Lee, T. R. Low-Density Self-Assembled Monolayers on Gold Derived from Chelating 2-Monoalkylpropane-1,3-dithiols. *Langmuir* **2000**, *16*, 541–548.

- (30) Park, J.-S.; Smith, A. C.; Lee, T. R. Loosely Packed Self-Assembled Monolayers on Gold Generated from 2-Alkyl-2-methylpropane-1,3-dithiols. *Langmuir* **2004**, *20*, 5829–5836.
- (31) Shon, Y.-S.; Lee, T. R. Desorption and Exchange of Self-Assembled Monolayers (SAMs) on Gold Generated from Chelating Alkanedithiols. *J. Phys. Chem. B* **2000**, *104*, 8192–8200.
- (32) Garg, N.; Carrasquillo-Molina, E.; Lee, T. R. Self-Assembled Monolayers Composed of Aromatic Thiols on Gold: Structural Characterization and Thermal Stability in Solution. *Langmuir* **2002**, *18*, 2717–2726.
- (33) Lee, H. J.; Jamison, A. C.; Yuan, Y.; Li, C.-H.; Rittikulsittichai, S.; Rusakova, I.; Lee, T. R. Robust Carboxylic Acid-Terminated Organic Thin Films and Nanoparticle Protectants Generated from Bidentate Alkanethiols. *Langmuir* **2013**, *29*, 10432–10439.
- (34) Tao, Y.-T.; Wu, C.-C.; Eu, J.-Y.; Lin, W.-L.; Wu, K.-C.; Chen, C.-H. Structure Evolution of Aromatic-Derivatized Thiol Monolayers on Evaporated Gold. *Langmuir* **1997**, *13*, 4018–4023.
- (35) Duan, L.; Garrett, S. J. An Investigation of Rigid p-Methylterphenyl Thiol Self-Assembled Monolayers on Au(111) Using Reflection-Absorption Infrared Spectroscopy and Scanning Tunneling Microscopy. *J. Phys. Chem. B* **2001**, *105*, 9812–9816.
- (36) Ulman, A.; Kang, J. F.; Shnidman, Y.; Liao, S.; Jordan, R.; Choi, G.-Y.; Zaccaro, J.; Myerson, A. S.; Rafailovich, M.; Sokolov, J.; Fleischer, C. Self-Assembled Monolayers of Rigid Thiols. *Rev. Mol. Biotechnol.* **2000**, *74*, 175–188.
- (37) Chang, S.-C.; Chao, I.; Tao, Y.-T. Structure of Self-Assembled Monolayers of Aromatic-Derivatized Thiols on Evaporated Gold and Silver Surfaces: Implication on Packing Mechanism. *J. Am. Chem. Soc.* **1994**, *116*, 6792–6805.
- (38) Tao, Y. T.; Lee, M. T.; Chang, S. C. Effect of Biphenyl and Naphthyl Groups on the Structure of Self-Assembled Monolayers: Packing, Orientation, and Wetting Properties. *J. Am. Chem. Soc.* **1993**, *115*, 9547–9555.
- (39) Shnidman, Y.; Ulman, A.; Eilers, J. E. Effect of Perturbing Strata on Chain Conformations and Ordering in Closely Packed Layered Structures of Chain Molecules. *Langmuir* **1993**, *9*, 1071–1081.
- (40) Srisombat, L.; Jamison, A. C.; Lee, T. R. Stability: A Key Issue for Self-Assembled Monolayers as Thin-Film Coatings and Nanoparticle Protectants. *Colloids Surf., A* **2011**, *390*, 1–19.
- (41) Strong, L.; Whitesides, G. M. Structures of Self-Assembled Monolayer Films of Organosulfur Compounds Adsorbed on Gold Single Crystals: Electron Diffraction Studies. *Langmuir* **1988**, *4*, 546–558.
- (42) Chidsey, C. E. D.; Liu, G. Y.; Rowntree, P.; Scoles, G. Molecular Order at the Surface of an Organic Monolayer Studied by Low Energy Helium Diffraction. *J. Chem. Phys.* **1989**, *91*, 4421–4423.
- (43) Bain, C. D.; Troughton, E. B.; Tao, Y. T.; Evall, J.; Whitesides, G. M.; Nuzzo, R. G. Formation of Monolayer Films by the Spontaneous Assembly of Organic Thiols From Solution onto Gold. *J. Am. Chem. Soc.* **1989**, *111*, 321–335.
- (44) Sieval, A. B.; Vleeming, V.; Zuilhof, H.; Sudhölter, E. J. R. An Improved Method for the Preparation of Organic Monolayers of 1-Alkenes on Hydrogen-Terminated Silicon Surfaces. *Langmuir* **1999**, *15*, 8288–8291.
- (45) Rozlosnik, N.; Gerstenberg, M. C.; Larsen, N. B. Effect of Solvents and Concentration on the Formation of a Self-Assembled Monolayer of Octadecylsiloxane on Silicon(001). *Langmuir* **2003**, *19*, 1182–1188.
- (46) Castner, D. G.; Hinds, K.; Grainger, D. W. X-Ray Photoelectron Spectroscopy Sulfur 2p Study of Organic Thiol and Disulfide Binding Interactions with Gold Surfaces. *Langmuir* **1996**, *12*, 5083–5086.
- (47) Carey, F. A.; Sundberg, R. J. *Advanced Organic Chemistry*, 3rd ed.; Plenum: New York, 1990.
- (48) Noh, J. G.; Jeong, Y. D.; Ito, E.; Hara, M. Formation and Domain Structure of Self-Assembled Monolayers by Adsorption of Tetrahydrothiophene on Au(111). *J. Phys. Chem. C* **2007**, *111*, 2691–2695.
- (49) Heeg, J.; Schubert, U.; Kuchenmeister, F. Mixed Self-Assembled Monolayers of Terminally Functionalized Thiols at Gold Surfaces Characterized by Angle Resolved X-ray Photoelectron Spectroscopy (ARXPS) Studies. *Fresenius' J. Anal. Chem.* **1999**, *365*, 272–276.
- (50) Laibinis, P. E.; Whitesides, G. M.; Allara, D. L.; Tao, Y. T.; Parikh, A. N.; Nuzzo, R. G. Comparison of the Structures and Wetting Properties of Self-Assembled Monolayers of n-Alkanethiols on the Coinage Metal Surfaces, Copper, Silver, and Gold. *J. Am. Chem. Soc.* **1991**, *113*, 7152–7167.
- (51) Porter, M. D.; Bright, T. B.; Allara, D. L.; Chidsey, C. E. D. Spontaneously Organized Molecular Assemblies. 4. Structural Characterization of n-Alkyl Thiol Monolayers on Gold by Optical Ellipsometry, Infrared Spectroscopy, and Electrochemistry. *J. Am. Chem. Soc.* **1987**, *109*, 3559–3568.
- (52) Troughton, E. B.; Bain, C. D.; Whitesides, G. M.; Nuzzo, R. G.; Allara, D. L.; Porter, M. D. Monolayer Films Prepared by the Spontaneous Self-Assembly of Symmetrical and Unsymmetrical Dialkyl Sulfides from Solution onto Gold Substrates: Structure, Properties, and Reactivity of Constituent Functional Groups. *Langmuir* **1988**, *4*, 365–385.
- (53) Ulman, A. Formation and Structure of Self-Assembled Monolayers. *Chem. Rev.* **1996**, *96*, 1533–1554.
- (54) Molecular models were performed using the Gaussview03, revision 3.07; Gaussian, Inc., Pittsburgh, PA. For simplicity, we assumed that the alkyl chains were fully extended and tilted $\sim 30^\circ$ from the surface normal. The following data were used: C–C $\sim 1.5 \text{ \AA}$, C–O $\sim 1.4 \text{ \AA}$, $\angle \text{CCC} \sim 109.5^\circ$, and $\angle \text{COC} \sim 110.8^\circ$.
- (55) Snyder, R. G.; Strauss, H. L.; Elliger, C. A. Carbon-Hydrogen Stretching Modes and the Structure of n-Alkyl Chains. 1. Long, Disordered Chains. *J. Phys. Chem.* **1982**, *86*, 5145–5150.
- (56) MacPhail, R. A.; Strauss, H. L.; Snyder, R. G.; Elliger, C. A. Carbon-Hydrogen Stretching Modes and the Structure of n-Alkyl Chains. 2. Long, All-Trans Chains. *J. Phys. Chem.* **1984**, *88*, 334–341.
- (57) Snyder, R. G.; Scherer, J. R. Band Structure in the Carbon-Hydrogen Stretching Region of the Raman Spectrum of the Extended Polymethylene Chain: Influence of Fermi Resonance. *J. Chem. Phys.* **1979**, *71*, 3221–3228.
- (58) Snyder, R. G.; Hsu, S. L.; Krimm, S. Vibrational Spectra in the Carbon-Hydrogen Stretching Region and the Structure of the Polymethylene Chain. *Spectrochim. Acta, Part A* **1978**, *34*, 395–406.
- (59) Whitesides, G. M.; Laibinis, P. E. Wet Chemical Approaches to the Characterization of Organic Surfaces: Self-Assembled Monolayers, Wetting, and the Physical-Organic Chemistry of the Solid-Liquid Interface. *Langmuir* **1990**, *6*, 87–96.
- (60) Bain, C. D.; Whitesides, G. M. Modeling Organic Surfaces with Self-Assembled Monolayers. *Angew. Chem.* **1989**, *101*, 522–528.
- (61) Schlenoff, J. B.; Li, M.; Ly, H. Stability and Self-Exchange in Alkanethiol Monolayers. *J. Am. Chem. Soc.* **1995**, *117*, 12528–12536.
- (62) Singhana, B.; Jamison, A. C.; Hoang, J.; Lee, T. R. Self-Assembled Monolayer Films Derived from Tridentate Cyclohexyl Adsorbates with Alkyl Tailgroups of Increasing Chain Length. *Langmuir* **2013**, *29*, 14108–14116.
- (63) Bhairamadgi, N. S.; Pujari, S. P.; Trovela, F. G.; Debrassi, A.; Khamis, A. A.; Alonso, J. M.; Al Zaharani, A. A.; Wennekes, T.; Al-Turaiif, H. A.; van Rijn, C.; Alhamed, Y. A.; Zuilhof, H. Hydrolytic and Thermal Stability of Organic Monolayers on Various Inorganic Substrates. *Langmuir* **2014**, *30*, 5829–5839.
- (64) Walczak, M. M.; Alves, C. A.; Lamp, B. D.; Porter, M. D. Electrochemical and X-Ray Photoelectron Spectroscopic Evidence for Differences in the Binding Sites of Alkanethiolate Monolayers Chemisorbed at Gold. *J. Electroanal. Chem.* **1995**, *396*, 103–114.
- (65) Bensebaa, F.; Ellis, T. H.; Badia, A.; Lennox, R. B. Probing the Different Phases of Self-Assembled Monolayers on Metal Surfaces: Temperature Dependence of the C-H Stretching Modes. *J. Vac. Sci. Technol., A* **1995**, *13*, 1331–1336.
- (66) Bensebaa, F.; Ellis, T. H.; Badia, A.; Lennox, R. B. Thermal Treatment of n-Alkanethiolate Monolayers on Gold, as Observed by Infrared Spectroscopy. *Langmuir* **1998**, *14*, 2361–2367.
- (67) Prathima, N.; Harini, M.; Rai, N.; Chandrashekhara, R. H.; Ayappa, K. G.; Sampath, S.; Biswas, S. K. Thermal Study of Accumulation of Conformational Disorders in the Self-Assembled

Monolayers of C8 and C18 Alkanethiols on the Au(111) Surface. *Langmuir* **2005**, *21*, 2364–2374.

(68) Greenler, R. G. Infrared Study of Adsorbed Molecules on Metal Surfaces by Reflection Techniques. *J. Chem. Phys.* **1966**, *44*, 310–335.

(69) Pan, S.; Belu, A. M.; Ratner, B. D. Self Assembly of 16-Mercapto-1-hexadecanol on Gold: Surface Characterization and Kinetics. *Mater. Sci. Eng., C* **1999**, *7*, 51–58.